Human Molecular Genetics, 1999, Vol. 8, No. 5 723–730

ARTICLE

Embryonic lethality and vascular defects in mice lacking the Notch ligand Jagged1

Yingzi Xue[1,2,+,‡], Xiang Gao[1,+,§], Claire E. Lindsell[3], Christine R. Norton[1], Bo Chang[1], Carol Hicks[3], Maureen Gendron-Maguire[1,¶], Elizabeth B. Rand[4], Gerry Weinmaster[3] and Thomas Gridley[1,*]

[1]The Jackson Laboratory, 600 Main Street, Bar Harbor, ME 04609-1500, USA, [2]Department of Biological Sciences, Columbia University, New York, NY 10027, USA, [3]Department of Biological Chemistry, UCLA School of Medicine, Los Angeles, CA 90024, USA and [4]Division of Gastroenterology and Nutrition, The Children's Hospital of Philadelphia, University of Pennsylvania School of Medicine, Philadelphia, PA 19104, USA

Received November 6, 1998; Revised and Accepted February 4, 1999

The Notch signaling pathway is an evolutionarily conserved intercellular signaling mechanism essential for embryonic development in mammals. Mutations in the human JAGGED1 (*JAG1*) gene, which encodes a ligand for the Notch family of transmembrane receptors, cause the autosomal dominant disorder Alagille syndrome. We have examined the *in vivo* role of the mouse *Jag1* gene by creating a null allele through gene targeting. Mice homozygous for the *Jag1* mutation die from hemorrhage early during embryogenesis, exhibiting defects in remodeling of the embryonic and yolk sac vasculature. We mapped the *Jag1* gene to mouse chromosome 2, in the vicinity of the Coloboma (*Cm*) deletion. Molecular and complementation analyses revealed that the *Jag1* gene is functionally deleted in the *Cm* mutant allele. Mice heterozygous for the *Jag1* null allele exhibit an eye dysmorphology similar to that of *Cm*/+ heterozygotes, but do not exhibit other phenotypes characteristic of *Cm*/+ mice or of humans with Alagille syndrome. These results establish the phenotype of *Cm*/+ mice as a contiguous gene deletion syndrome and demonstrate that *Jag1* is essential for remodeling of the embryonic vasculature.

INTRODUCTION

The Notch signaling pathway is an evolutionarily conserved intercellular signaling mechanism and mutations in its components disrupt cell fate specification and embryonic development in organisms as diverse as insects, nematodes and mammals (reviewed in refs 1–3). Recent work has established that two human diseases are caused by mutations in components of the Notch signaling pathway. Mutations in the *NOTCH3* gene cause cerebral autosomal dominant arteriopathy with subcortical infarcts and leukoencephalopathy (CADASIL; OMIM 125310), an inherited vascular dementia syndrome (4). Mutations in the *JAG1* gene, which encodes a ligand for Notch family receptors (5), cause Alagille syndrome (6,7). Alagille syndrome (OMIM 118450) is a pleiotropic developmental disorder that is one of the major forms of chronic liver disease in childhood. Alagille syndrome exhibits autosomal dominant inheritance and is characterized by neonatal jaundice and a paucity of intrahepatic bile ducts. Accompanying features of this syndrome include congenital heart defects, skeletal defects, ophthalmological abnormalities and characteristic facial appearance (reviewed in ref. 8). The mutations originally found in the *JAG1* gene in Alagille syndrome patients were inactivating mutations, generally leading to premature truncation of the JAGGED1 protein (6,7). Surveys of the types and frequency of *JAG1* mutation in Alagille syndrome patients revealed that patients with large deletions encompassing the entire *JAG1* gene had the same phenotype as patients with intragenic *JAG1* mutations, suggesting that haploinsufficiency for the *JAG1* gene was the cause of Alagille syndrome (9,10). In this paper, we have examined the role of the mouse *Jag1* gene by creating a null allele and have characterized embryos and mice homozygous and heterozygous for this mutation.

*To whom correspondence should be addressed. Tel: +1 207 288 6237; Fax: +1 207 288 6077; Email: gridley@jax.org
Present addresses: ‡Skirball Institute of Biomolecular Medicine, New York University Medical Center, New York, NY 10016, USA; §UNC Neuroscience Center, University of North Carolina, Chapel Hill, NC 27599, USA; ¶Schering-Plough Research Institute, Kenilworth, NJ 07033, USA
+These authors contributed equally to this manuscript

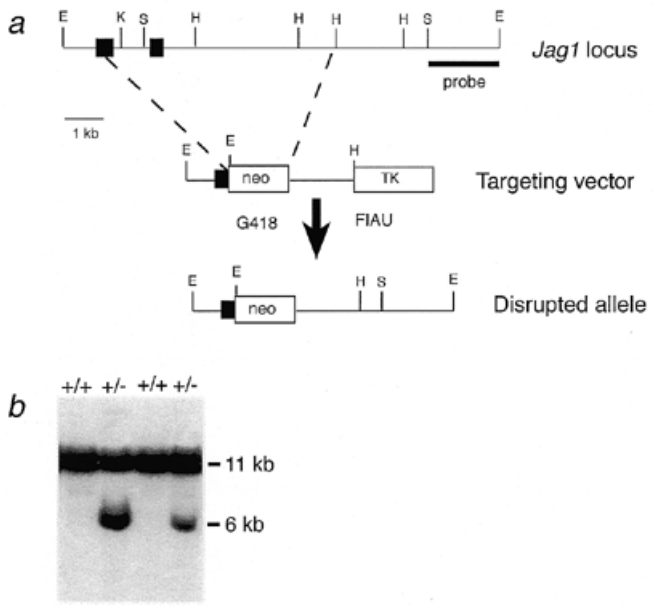

Figure 1. Targeted disruption of the mouse *Jag1* gene. (**a**) Targeting scheme. The upper line shows the genomic organization of a portion of the *Jag1* gene. Exons are indicated by black boxes. Additional exons are present 3′ of the exons indicated. The middle line represents the structure of the targeting vector. The bottom line shows the predicted structure of the *Jag1* locus following homologous recombination of the targeting vector. Probes used for Southern blot analysis are indicated. Restriction enzymes: E, *Eco*RI; H, *Hin*dIII; K, *Kpn*I; S, *Stu*I. (**b**) DNA isolated from embryos of the intercross of *Jag1*^{dDSL}/+ heterozygous mice was digested with *Eco*RI, blotted and hybridized with the indicated probe. Genotypes of progeny are indicated at the top of the lane.

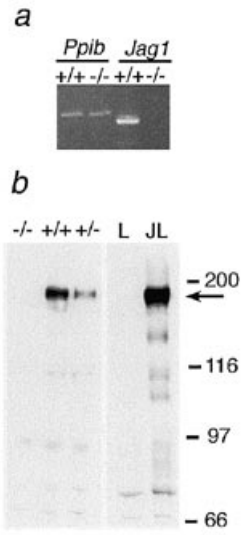

Figure 2. Analysis of *Jag1* gene products by RT–PCR and western blot. (**a**) RT–PCR analysis of RNA isolated from embryos at E10. Primers used were specific for *Jag1* and for peptidylprolyl isomerase B (*Ppib*) (used as a positive control). (**b**) Western blot analysis. The three left lanes are E10.5 embryo extracts with the indicated genotypes; the right two lanes are extracts from control and *Jag1* transfected cell lines. The arrow indicates the size of full-length Jagged1 protein. L, L cells; JL, L cells transfected with *Jag1* expression plasmid.

RESULTS

Disruption of the mouse *Jag1* gene

To analyze the *in vivo* role of the *Jag1* gene, a targeting vector was constructed that deletes 5 kb of genomic sequence near the 5′-end of the *Jag1* gene (Fig. 1a). The targeted allele deletes the C-terminal portion of the DSL domain, which is required for interaction of ligands with Notch family receptors (2,11). We refer to this mutant allele as *Jag1*^{dDSL}. The linearized targeting vector was electroporated into embryonic stem (ES) cells and germline transmission of the *Jag1*^{dDSL} allele was obtained for two targeted clones (Fig. 1b). Mice heterozygous for the *Jag1*^{dDSL} mutant allele were grossly normal, viable and fertile. RT–PCR and western blot analyses indicated that no *Jag1* RNA or protein was detectable in *Jag1*^{dDSL}/*Jag1*^{dDSL} homozygous mutant embryos (Fig. 2).

Jag1^{dDSL} homozygous mutant embryos exhibit defects in vascular remodeling

To examine whether animals homozygous for the *Jag1*^{dDSL} mutation were viable, heterozygous F_1 animals were intercrossed and genotypes of the F_2 progeny determined 2–3 weeks after birth. No homozygotes were detected, indicating that the *Jag1*^{dDSL} allele is a recessive lethal mutation. To determine when homozygous mutant embryos were dying, embryos were isolated from timed matings. At embryonic day (E)10.5, *Jag1*^{dDSL}/*Jag1*^{dDSL} homozygotes could be identified easily due to hemorrhaging and the presence of yolk sacs lacking large blood vessels (Fig. 3a and b). Histological analysis confirmed widespread hemorrhage, in particular in the cranial mesenchyme (Fig. 3c and d). When isolated at E11.5, homozygous mutant embryos were either completely resorbed or were severely necrotic, while at E9.5 homozygous mutant embryos could not usually be distinguished from wild-type and heterozygous littermates (data not shown).

We visualized the vascular network of *Jag1*^{dDSL}/*Jag1*^{dDSL} embryos and littermate controls in whole mount preparations by staining with a monoclonal antibody to platelet endothelial cell adhesion molecule-1 (PECAM-1), which is a specific marker for vascular endothelial cells (12). Defects in formation of the vascular system were observed both in the yolk sac and in the embryo of *Jag1*^{dDSL}/*Jag1*^{dDSL} homozygotes. Large vitelline blood vessels were present in the yolk sacs of control littermates, but large blood vessels were not present in the yolk sacs of *Jag1*^{dDSL}/*Jag1*^{dDSL} homozygous mutant embryos (Fig. 3e and f). The cranial region of the homozygous mutant embryos also exhibited vascular defects. The vascular network overlying the forebrain of the mutant embryos was not as intricate as that of heterozygous and wild-type littermates (Fig. 3g and h). Large blood vessels of the head had an abnormal appearance and a reduced diameter in the *Jag1*^{dDSL}/*Jag1*^{dDSL} homozygous mutant embryos (Fig. 3i and j).

Several groups have previously documented expression of the *Jag1* gene (also referred to as the *Serrate1* gene) in blood vessels in chick and mouse embryos (13–15). However, *Jag1* expression in cranial blood vessels that appear to be the first site of

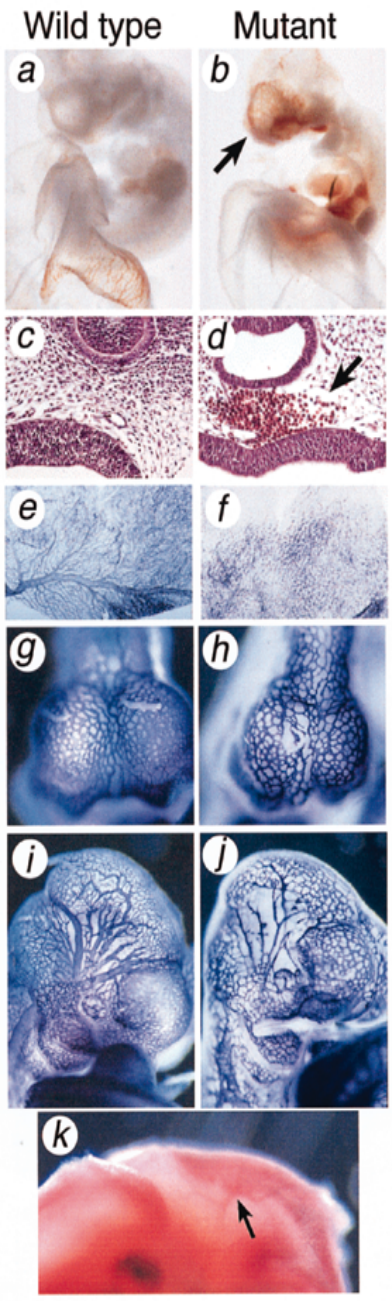

Figure 3. Vascular defects in *Jag1*^{dDSL} mutant homozygotes. (a–j) Wild-type embryos are shown in the left column, *Jag1*^{dDSL}/*Jag1*^{dDSL} homozygous mutant embryos in the right column. (**a** and **b**) Whole mounts of E10.5 embryos and yolk sacs. Arrow indicates cranial hemorrhage in the mutant embryo. The yolk sac of the mutant is pale and lacks obvious large blood vessels. (**c** and **d**) Histological analysis reveals a large hemorrhage (arrow) adjacent to the optic vesicle in the mutant embryo. (e–j) PECAM-1 stained yolk sacs and embryos. (**e** and **f**) The mutant yolk sac has failed to remodel the primary vascular plexus to form large blood vessels. (**g** and **h**) The vascular network overlying the forebrain vesicles is less intricate in the mutant embryo. (**i** and **j**) The vessels in the head of the mutant embryo have a reduced diameter and an abnormal appearance. (**k**) Whole mount *in situ* hybridization with a *Jag1* antisense riboprobe of an E10.5 wild-type embryo. *Jag1* expression can be observed in cranial blood vessels (arrow). A 'salt and pepper' pattern of *Jag1* expression in the neuroepithelium is also observed.

hemorrhage in *Jag1*^{dDSL}/*Jag1*^{dDSL} homozygous mutant embryos had not been reported. *In situ* hybridization of E10.5 wild-type embryos revealed *Jag1* expression in cranial blood vessels (Fig. 3k).

Jag1^{dDSL} homozygous mutant embryos do not exhibit defects in somitogenesis

Recent work has demonstrated that mutations in components of the Notch signaling pathway cause defects in segmentation and somite formation in mice (16–21). Since the *Jag1* gene is expressed in the forming somite (13,21,22), we analyzed *Jag1*^{dDSL}/*Jag1*^{dDSL} homozygous mutant embryos with several markers expressed in somites and in unsegmented paraxial mesoderm, including the genes *Dll1* (23), *Dll3* (24), *Lunatic fringe* (*Lfng*; 21) and *Uncx4.1* (25). This analysis revealed no detectable defects in segmentation in the *Jag1*^{dDSL}/*Jag1*^{dDSL} mutant embryos (Fig. 4).

The *Jag1* gene is deleted in the Coloboma deletion

We mapped the chromosomal location of the *Jag1* gene by interspecific backcross analysis to distal chromosome 2 (Fig. 5), close to the semidominant Coloboma (*Cm*) mutation (26). *Cm*/+ mice display several defects, including ophthalmic dysmorphology (e.g. iris colobomas), head bobbing, circling and profound hyperactivity (27). Molecular analysis has revealed that *Cm* is a 1–2 cM deletion (26).

To test whether the *Jag1* gene mapped within the *Cm* deletion, we crossed a male *Cm*/+ hemizygote with *Jag1*^{dDSL}/+ female heterozygotes and isolated embryos at E10.5. Four out of 15 embryos from two different litters exhibited cranial hemorrhaging identical to *Jag1*^{dDSL}/*Jag1*^{dDSL} homozygous mutant embryos (Fig. 6b–d). When yolk sac DNA isolated from these abnormal embryos was genotyped with allele-specific PCR primers, the *Jag1*^{dDSL} mutant allele-specific primers amplified a band of the correct size, but the *Jag1* wild-type allele-specific primers did not amplify any band (Fig. 6a). This indicated that the portion of the *Jag1* gene defined by our wild-type allele-specific PCR primers (the region encoding the DSL domain of the JAG1 protein) is deleted on the *Cm* chromosome. We have not determined if the entire coding sequence of the *Jag1* gene is deleted on the *Cm* chromosome.

In a previous study, Theiler and Varnum (28) had examined embryos from the intercross of *Cm*/+ heterozygotes between E6.0 and E9.5 and concluded from this analysis that *Cm*/*Cm* homozygotes died before day 6 of gestation. However, *Jag1*^{dDSL}/*Jag1*^{dDSL} homozygous mutant embryos are generally not apparent phenotypically until ~E10.5. We therefore examined embryos from the intercross of *Cm*/+ heterozygotes at E10.5. We isolated 38 embryos from five different litters of *Cm*/+ intercrosses. Ten out of 38 (26%) of these embryos were hemorrhagic (Fig. 6e) and PCR analysis indicated that these embryos were *Cm*/*Cm* homozygotes (data not shown; see Materials and Methods). These results demonstrate that *Cm*/*Cm* homozygous mutant embryos do not die prior to E6, but die around E10.5 from vascular defects similar to those exhibited by *Jag1*^{dDSL}/*Jag1*^{dDSL} homozygous mutant embryos.

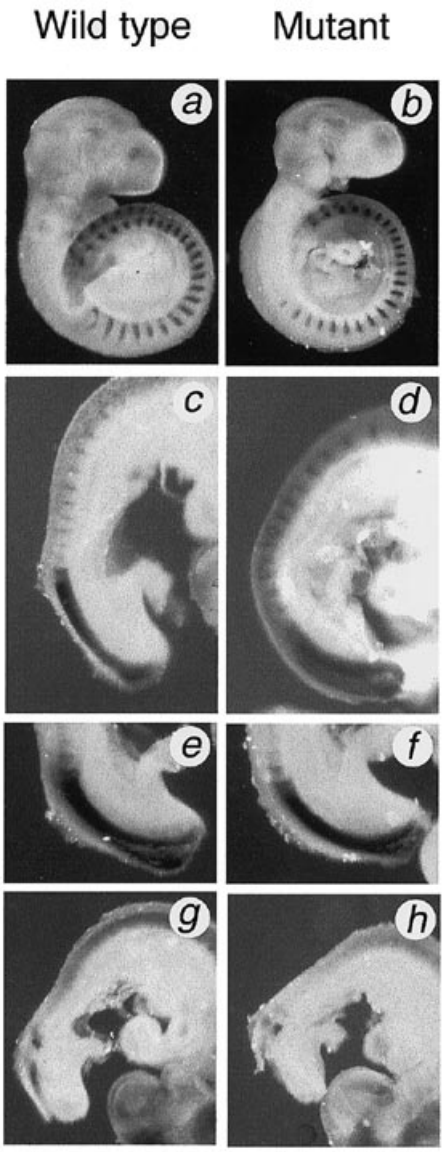

Figure 4. *Jag1*^{dDSL} mutant homozygotes do not exhibit defects in segmentation. Whole mount *in situ* hybridization with the indicated probes to embryos isolated at E9.5. Wild-type embryos are shown in the left column, *Jag1*^{dDSL}/*Jag1*^{dDSL} homozygous mutant embryos in the right column. (**a** and **b**) *Uncx4.1* probe; (**c** and **d**) *Dll1* probe; (**e** and **f**) *Dll3* probe; (**g** and **h**) *Lfng* probe.

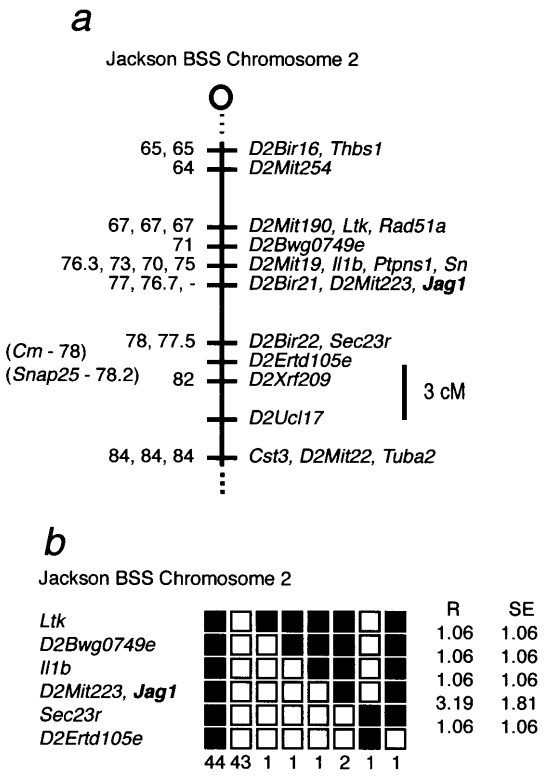

Figure 5. *Jag1* chromosomal mapping. (**a**) Localization of *Jag1* to mouse chromosome 2. A partial chromosome 2 linkage map showing the location of *Jag1* in relation to linked markers is shown. To the left of the chromosome is shown the cM position for these loci, as well as the cM positions for two loci not mapped in this cross, *Cm* and *Snap25*. (**b**) Haplotype figure showing part of chromosome 2 with loci linked to *Jag1*. The black boxes represent the C57BL6/JEi allele and the white boxes the SPRET/Ei allele. The percentage recombination (R) between adjacent loci is given to the right of the figure, with the standard error (SE).

Phenotypic effects in *Jag1*^{dDSL}/+ heterozygous mice

We examined *Jag1*^{dDSL}/+ adult heterozygotes for phenotypic abnormalities, since both Alagille syndrome in humans and phenotypes associated with the *Cm* deletion in mice are inherited as semidominant mutations. The *Jag1*^{dDSL}/+ mice exhibited an eye dysmorphology similar to that of *Cm*/+ mice (Table 1 and Fig. 7). The penetrance of the eye dysmorphology phenotype in *Jag1*^{dDSL}/+ mice was high (~80%) on a mixed genetic background and increased to 100% on a predominantly C57BL/6J background (Table 1). However, the *Jag1*^{dDSL}/+ heterozygotes did not appear to display the head bobbing, circling and hyperactivity characteristic of *Cm*/+ mice (27). *Jag1*^{dDSL}/+ adult heterozygotes (n = 10) were examined for other phenotypic abnormalities associated with Alagille syndrome in humans (e.g. defects of the liver, heart and axial skeleton), but no defects in these structures were observed in the *Jag1*^{dDSL}/+ mice.

Table 1. Summary of eye defects in *Jag1*^{dDSL}/+ heterozygous mice

Genetic background	Genotype	No. with eye defects/total	%
~80% C57BL/6J	+/+	0/25	0
	Jag1^{dDSL}/+	25/25	100
Mixed 129/B6/FVB	+/+	0/19	0
	Jag1^{dDSL}/+	13/16	81

Eye defects included iris colobomas, irregular or off-center pupils and corneal opacity.

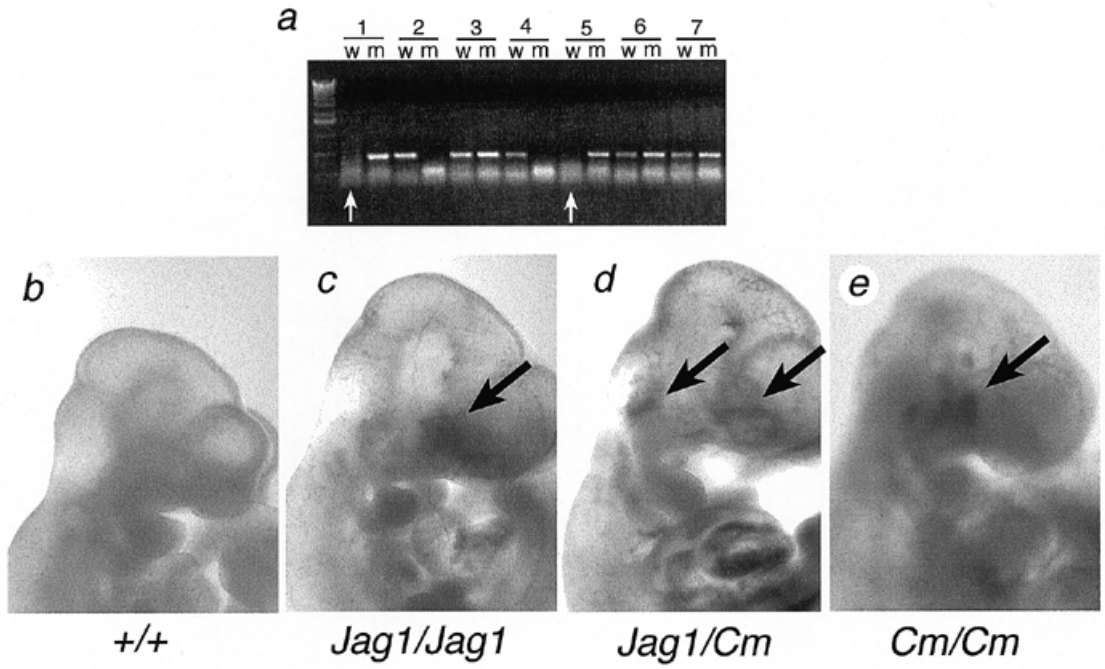

Figure 6. Deletion of the *Jag1* gene on the *Cm* chromosome. (**a**) PCR genotyping of embryos from the intercross of a *Cm*/+ male and a $Jag1^{dDSL}$/+ female. White arrows indicate embryos (nos 1 and 5) that did not amplify the wild-type *Jag1* band. These embryos were hemorrhagic; all other embryos in this litter had a wild-type morphology. (b–d) Whole mount morphology of embryos isolated at E10.5. (**b**) Wild-type; (**c**) $Jag1^{dDSL}/Jag1^{dDSL}$; (**d**) $Jag1^{dDSL}/Cm$; (**e**) *Cm*/*Cm*. Black arrows indicate areas of hemorrhage in $Jag1^{dDSL}/Jag1^{dDSL}$, $Jag1^{dDSL}/Cm$ and *Cm*/*Cm* embryos.

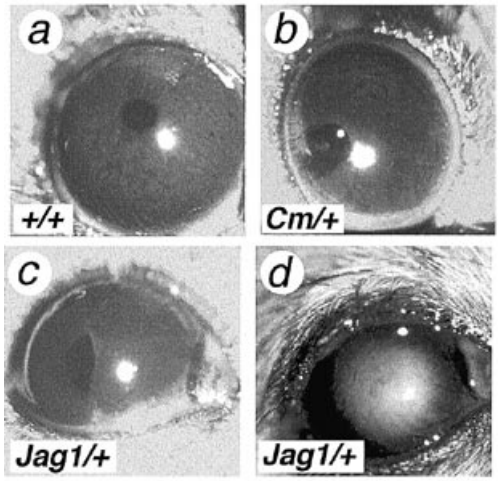

Figure 7. Eye dysmorphologies in $Jag1^{dDSL}$/+ and *Cm*/+ mutant heterozygotes. (**a**) Wild-type; (**b**) iris coloboma in *Cm*/+ heterozygote; (**c**) iris coloboma in $Jag1^{dDSL}$/+ heterozygote; (**d**) corneal opacity in $Jag1^{dDSL}$/+ heterozygote. The white dot in each eye is a reflection from the lamp used for illumination.

DISCUSSION

Defects in vascular remodeling in $Jag1^{dDSL}$ homozygous mutant embryos

In this report we have demonstrated that the Notch ligand encoded by the *Jag1* gene plays an essential role during embryonic development in mice. Mice homozygous for a targeted null mutation of the *Jag1* gene die at E10 due to vascular defects. During the early stages of vascular development in both the embryo and the yolk sac, endothelial cell precursors differentiate and coalesce into a network of homogeneously sized primitive blood vessels (the primary vascular plexus) in a process termed vasculogenesis. This primary vascular plexus is then remodeled into the large and small vessels of the mature vascular system by the process of angiogenesis (29,30). In the yolk sac of $Jag1^{dDSL}/Jag1^{dDSL}$ homozygous mutant embryos, the primary vascular plexus appeared to form normally, indicating that there were no apparent defects in vasculogenesis in the homozygous mutants. However, the $Jag1^{dDSL}/Jag1^{dDSL}$ homozygous mutant embryos failed to remodel the primary vascular plexus to form the large vitelline blood vessels, a process that occurs by angiogenesis. The cranial region of the homozygous mutant embryos also exhibited a defect in vascular remodeling. The vascular network overlying the forebrain of the mutant embryos was not as intricate as that of control littermates and the large blood vessels of the head had an abnormal appearance and a reduced diameter. These abnormalities suggest that the $Jag1^{dDSL}/Jag1^{dDSL}$ homozygous mutant embryos exhibit defects in angiogenic vascular remodeling both in the yolk sac and in the embryo.

Zimrin *et al.* have previously demonstrated a connection between *Jag1* expression and angiogenesis (31). They isolated the human *Jag1* cDNA in a differential display screen for genes induced in an *in vitro* angiogenesis model and also showed that administration of *Jag1* antisense oligonucleotides could modulate *in vitro* angiogenesis (31). Our results extend these findings by demonstrating that expression of the *Jag1* gene plays an important role in vascular development during embryogenesis in

mice, in particular during angiogenic vascular remodeling. Taken together with the finding that mutations of the human *Notch3* gene cause the systemic vascular disease CADASIL (4), these results indicate that components of the Notch signaling pathway are essential both for vascular development in embryos and maintenance of a healthy vascular system in adults.

Absence of somite defects in *Jag1*^{dDSL} homozygous mutant embryos

Recent work has demonstrated that mutations in components of the Notch signaling pathway cause defects in somite formation in mice. Notch pathway mutants exhibiting defects in somitogenesis include the genes encoding the *Notch1* receptor (16,17), the ligands *Dll1* (18) and *Dll3* (19) and *Lfng* (20,21), which encodes a secreted protein that regulates Notch signaling (22,32). We analyzed *Jag1*^{dDSL}/*Jag1*^{dDSL} homozygous mutant embryos with several markers expressed in somites and in unsegmented paraxial mesoderm and found no detectable defects in segmentation in the homozygous mutant embryos. This result supports our previous finding that expression of the *Jag1* gene in the forming somite is unaffected in *Lfng*$^{-/-}$ mutant embryos (21). We have also demonstrated previously that mice homozygous for a null mutation of the related *Jagged2* (*Jag2*) gene, while displaying a variety of phenotypic defects, exhibit no defects in somite formation (33). These findings reveal a division of function among the Notch family ligands. Notch signaling mediated by the Delta family ligands encoded by the *Dll1* and *Dll3* genes is essential for proper somite formation, but signaling mediated by the Serrate family ligands encoded by the *Jag1* and *Jag2* genes is not required for somitogenesis in mice.

Gene dosage-sensitive phenotypic effects in *Jag1*^{dDSL}/+ heterozygous mice

While our RT–PCR and western blot data indicated that the *Jag1*^{dDSL} allele is most likely a null (amorphic) allele, the most stringent genetic test to determine whether a particular mutation is a null allele is to test that mutation over a deletion of the locus in question (34). Our finding that at least a portion of the *Jag1* gene is deleted on the *Cm* mutant chromosome permitted us to perform this classic genetic test. Since the phenotype of the *Jag1*^{dDSL}/*Cm* mutant embryos appeared identical to that of *Jag1*^{dDSL}/*Jag1*^{dDSL} homozygotes, this analysis confirmed that the targeted *Jag1*^{dDSL} mutation is a null allele.

Since both Alagille syndrome in humans and phenotypes associated with the *Cm* deletion in mice are inherited as semidominant mutations, we examined *Jag1*^{dDSL}/+ adult heterozygotes for phenotypic abnormalities. The *Jag1*^{dDSL}/+ mice exhibited an eye dysmorphology similar to that of *Cm*/+ mice, but did not appear to display the head bobbing, circling and hyperactivity characteristic of *Cm*/+ mice (27). Similarly, Alagille syndrome patients often display ophthalmological abnormalities, typically including anterior chamber defects and posterior embryotoxon (8). The ophthalmological abnormalities displayed by the *Jag1*^{dDSL}/+ adult heterozygotes are somewhat different in type and are more severe than the abnormalities typically displayed by Alagille syndrome patients. Both *Jag1*^{dDSL}/+ and *Cm*/+ mice exhibit iris colobomas (Fig. 7). The iris, at its periphery, is continuous with the ciliary body. During development of the eye, the *Jag1* gene is expressed in the ciliary body (35,36). While we do not currently understand at a mechanistic level how reduction of *Jag1* gene dosage leads to the formation of iris colobomas, this phenotype correlates well with the pattern of expression of the *Jag1* gene during eye development.

In contrast to the presence of eye dysmorphologies in the *Jag1*^{dDSL}/+ heterozygotes, these mice did not appear to exhibit other phenotypic abnormalities (e.g. defects of the liver, heart and axial skeleton) associated with Alagille syndrome in humans. Phenotypes sensitive to gene dosage are characteristic of mutations of Notch pathway components in *Drosophila* (reviewed in ref. 37). The eye phenotype of the *Jag1*^{dDSL}/+ mice is the first documented instance of a gene dosage-sensitive phenotype in any of the Notch pathway mutants in mice. However, the *Jag1*^{dDSL}/+ mice do not appear to represent a good animal model for Alagille syndrome.

The phenotypes of *Cm*/+ mice constitute a contiguous gene deletion syndrome

Several human disorders (termed contiguous gene deletion syndromes) are associated with either cytogenetically detectable or submicroscopic chromosomal deletions (38). In mice, the *Cm* deletion has been shown to encompass the genes encoding phospholipase C isoform β-1 and the synaptosome-associated protein (25 kDa; *Snap25*) (26). Expression of a transgene encoding the SNAP25 protein rescues the hyperactivity of *Cm*/+ hemizygotes, but not the ophthalmic dysmorphology or head bobbing (27). Our molecular and genetic data indicate that the *Cm* deletion also encompasses at least a portion of the *Jag1* gene and that loss of the *Jag1* gene is responsible for the ophthalmic dysmorphology of *Cm*/+ hemizygotes. These data indicate that the phenotype of *Cm*/+ mice constitutes a contiguous gene deletion syndrome.

MATERIALS AND METHODS

Isolation of genomic and cDNA clones and targeting vector construction

Genomic clones of the *Jag1* gene were obtained by screening a P1 genomic library made from genomic DNA of 129/Sv strain mouse embryonic stem cells (Genome Systems, St Louis, MO) with PCR primers corresponding to sequences specific to the mouse *Jag1* cDNA. Positive P1 clones were analyzed by restriction mapping and Southern hybridization. Fragments that hybridized to *Jag1* cDNA clones were subcloned and the exon–intron organization of part of the *Jag1* gene was determined by nucleotide sequencing.

The targeting vector was constructed from an 11 kb genomic subclone of the *Jag1* gene. The 3′ arm was a 2.3 kb *Hin*dIII genomic fragment that was subcloned downstream of a PGK-*neo* expression cassette (39). To construct the 5′ arm, an oligonucleotide (5′-AAGCAATTGCGCCAAAGCCATAG-3′) complementary to a sequence in the middle of the exon encoding the DSL domain of the JAG1 protein was used as a PCR primer for amplification on a *Jag1* genomic subclone. The amplified fragment was then subcloned upstream of the PGK-*neo* cassette. This disrupted the exon encoding the DSL domain and resulted in the deletion of a 5.0 kb genomic fragment containing the exons encoding the C-terminal half of the DSL domain and half of the first EGF repeat of the JAG1 protein. In this paper, we refer to this allele as *Jag1*^{dDSL} (the nomenclature for this allele assigned by

the International Committee on Standardized Genetics Nomenclature for Mice is *Jag1*^{tm1Grid}). A HSV-*tk* cassette (40) was also introduced to allow negative selection against random integration of the targeting vector.

Electroporation, selection and screening of ES cells and mouse genotyping

CJ7 ES cells were electroporated with 25 µg of linearized targeting vector, selected, screened and injected into blastocysts from C57BL/6J mice as previously described (41). Animals were genotyped by Southern blot analysis or by PCR. PCR primers for the *Jag1* wild-type allele were JG1 (5′-TCTCACTCAGGCATGATAAACC-3′) and JG2 (5′-TAACGGGGACTCCGGACAGGG-3′). Primers for the *Jag1*^{dDSL} allele were JG1 and JG4 (5′-GGTGCTGTCCATCTGCACGAG-3′). For RT–PCR, the *Jag1* primers were JGRT1 (5′-AGTGCCCAGAGCTTGAACCG-3′) and JGRT2 (5′-CTAAGGCTGCCATCACCATTAGG-3′). Control primers for peptidylprolyl isomerase B (*Ppib*) were (5′-ATATGAAGGTGCTCTTCGCCGCCG-3′) and (5′-CATTGGTGTCTTTGCCTGCATTGGC-3′).

Examination of *Cm*/*Cm* embryos

Male *Cm*/+ heterozygous mice on the C3H/HeSnJ background were backcrossed for two generations to C57BL/6J mice. *Cm*/+ heterozygous adult progeny were genotyped by examination for the presence of iris colobomas. These *Cm*/+ heterozygotes were intercrossed, and progeny were isolated at E10.5. Embryos were fixed for morphological analysis and DNA was prepared from the yolk sac of each embryo. Yolk sac DNA was examined for the presence of the wild-type *Jag1* gene by allele-specific PCR using the primers JG1 and JG2 (see above). Primers for the wild-type *Notch2* gene, which is located on chromosome 3 (42), were used as a positive control for DNA integrity. Primers for the *Notch2* wild-type allele were (5′-TCTCCATATTGATGAGCCATGC-3′) and (5′-CCAGTGTGCCACAGGTAAGTG-3′).

Western blot analysis

Polyclonal antiserum (J59) specific for the cytoplasmic domain of rat JAG1 was raised by immunizing a rabbit with a bacterially expressed protein consisting of amino acids 1101–1219 inclusive of rat JAG1 fused to glutathione *S*-transferase. Embryo lysates (at E10.5) were separated on 8% SDS–PAGE gels and transferred to PVDF membrane. The membrane was incubated with affinity purified J59 antiserum and with goat anti-rabbit–horseradish peroxidase conjugate (Cappel, Durham, NC). The horseradish peroxidase signal was detected using chemiluminescence substrate (ECL; Amersham, Arlington Heights, IL).

Histology, *in situ* hybridization and immunohistochemistry

Embryos were dissected and DNA was prepared from the yolk sacs or tails for genotyping. Embryos for histological analysis were fixed in Bouin's fixative. Fixed embryos were dehydrated through graded alcohols, embedded in paraffin, sectioned and stained with hematoxylin and eosin. Embryos for *in situ* hybridization were fixed overnight at 4°C in 4% paraformaldehyde in phosphate-buffered saline (PBS). Embryos for immunohistochemistry were fixed in 4% paraformaldehyde in PBS and stained with a monoclonal anti-PECAM-1 antibody (Pharmingen, San Diego, CA). For analysis of *Jag1*^{dDSL}/+ heterozygous adult mice, animals were examined with a slit lamp for eye defects. Livers and hearts from these *Jag1*^{dDSL}/+ heterozygotes (which all displayed eye defects; n = 10 *Jag1*^{dDSL}/+ heterozygotes) and from age-matched littermate controls were dissected, fixed in Bouin's fixative and sectioned. Skeletons were examined by X-ray analysis.

Chromosomal localization

We determined the chromosomal location of the *Jag1* gene by interspecific backcross analysis. C57BL/6J and *M.spretus* DNAs were digested with several enzymes and analyzed for informative restriction fragment length polymorphisms (RFLPs) by Southern blotting using a *Jag1* genomic probe (a 2.2 kb *Eco*RI–*Stu*I fragment). An *Eco*RV RFLP was then used to analyze Southern blots of *Eco*RV-digested DNA from 94 N_2 progeny from the cross (C57BL/6JEi×SPRET/Ei)F_1×SPRET/Ei from the Jackson Laboratory BSS interspecific backcross panel (43). The presence or absence of the C57BL/6J-specific *Eco*RV fragment was followed in the backcross mice. Raw typing data for this cross are available at http://www.jax.org/resources/documents/cmdata . Centimorgan postitions for *Cm* and *Snap25* (which have not been mapped in the Jackson BSS backcross) were obtained from the Mouse Genome Database (http://www.informatics.jax.org/locus.html).

ACKNOWLEDGEMENTS

We thank M. Wilson for helpful discussions, L. Rowe and M. Barter of the Jackson Laboratory Backcross DNA Panel Mapping Resource for advice and for providing the chromosome mapping figures, one of the anonymous reviewers for suggesting an additional experiment and S. Ackerman, M. Davisson and A. Gossler for comments on the manuscript. This work was supported by grants from the NIH (NS36437 and HD34883 to T.G.; NS31885 to G.W.; EY07758 to B.C.) and the March of Dimes Foundation (1-FY97-0193 to T.G.; 5-FY94-0757 to G.W.). This work was also supported by a grant from the National Cancer Institute (CA34196) to the Jackson Laboratory.

REFERENCES

1. Artavanis-Tsakonas, S., Matsuno, K. and Fortini, M.E. (1995) Notch signaling. *Science*, **268**, 225–232.
2. Weinmaster, G. (1997) The ins and outs of Notch signaling. *Mol. Cell. Neurosci.*, **9**, 91–102.
3. Gridley, T. (1997) Notch signaling in vertebrate development and disease. *Mol. Cell. Neurosci.*, **9**, 103–108.
4. Joutel, A., Corpechot, C., Ducros, A., Vahedi, K., Chabriat, K.H., Mouton, P., Alamowitch, S., Domenga, V., Cécillion, M., Maréchal, E., Maciazek, J., Vayssiére, C., Cruaud, C., Cabanis, E.-A., Ruchoux, M.M., Weissenbach, J., Bach, J.F., Bousser, M.G. and Tournier-Lasserve, E. (1996) Notch3 mutations in CADASIL, a hereditary adult-onset condition causing stroke and dementia. *Nature*, **383**, 707–710.
5. Lindsell, C.E., Shawber, C.J., Boulter, J. and Weinmaster, G. (1995) Jagged: a mammalian ligand that activates Notch1. *Cell*, **80**, 909–917.
6. Li, L., Krantz, I.D., Deng, Y., Genin, A., Banta, A.B., Collins, C.C., Qi, M., Trask, B.J., Kuo, W.L., Cochran, J., Costa, T., Pierpont, M.E., Rand, E.B., Piccoli, D.A., Hood, L. and Spinner, N.B. (1997) Alagille syndrome is caused by mutations in human *Jagged1*, which encodes a ligand for Notch1. *Nature Genet.*, **16**, 243–251.
7. Oda, T., Elkahloun, A.G., Pike, B.L., Okajima, K., Krantz, I.D., Genin, A., Piccoli, D.A., Meltzer, P.S., Spinner, N.B., Collins, F.S. and Chandrasekharappa, S.C. (1997) Mutations in the human *Jagged1* gene are responsible for Alagille syndrome. *Nature Genet.*, **16**, 235–242.

8. Krantz, I.D., Piccoli, D.A. and Spinner, N.B. (1997) Alagille syndrome. *J. Med. Genet.*, **34**, 152–157.
9. Krantz, I.D., Colliton, R.P., Genin, A., Rand, E.B., Li, L., Piccoli, D.A. and Spinner, N.B. (1998) Spectrum and frequency of *Jagged1* (*JAG1*) mutations in Alagille syndrome patients and their families. *Am. J. Hum. Genet.*, **62**, 1361–1369.
10. Yuan, Z.-R., Kohsaka, T., Ikegaya, T., Suzuki, T., Okano, S., Abe, J., Kobayashi, N. and Yamada, M. (1998) Mutational analysis of the *Jagged1* gene in Alagille syndrome families. *Hum. Mol. Genet.*, **7**, 1363–1369.
11. Muskavitch, M.A.T. (1994) Delta-Notch signaling and *Drosophila* cell fate choice. *Dev. Biol.*, **166**, 415–430.
12. Baldwin, H.S., Shen, H.M., Yan, H.C., De Lisser, H.M., Chung, A., Mickanin, C., Trask, T., Kirschbaum, N.E., Newman, P.J., Albeda, S.M. and Buck, C.A. (1994) Platelet endothelial cell adhesion molecule-1 (PECAM-1/CD31): alternatively spliced, functionally distinct isoforms expressed during mammalian cardiovascular development. *Development*, **120**, 2539–2553.
13. Mitsiadis, T.A., Henrique, D., Thesleff, I. and Lendahl, U. (1997) Mouse *Serrate-1* (*Jagged1*): expression in the developing tooth is regulated by epithelial–mesenchymal interactions and fibroblast growth factor-4. *Development*, **124**, 1473–1483.
14. Myat, A., Henrique, D., Ish-Horowicz, D. and Lewis, J. (1996) A chick homologue of *Serrate* and its relationship with *Notch* and *Delta* homologues during central neurogenesis. *Dev. Biol.*, **174**, 233–247.
15. Vargesson, N., Patel, K., Lewis, J. and Tickle, C. (1998) Expression patterns of *Notch1*, *Serrate1*, *Serrate2* and *Delta1* in tissues of the developing chick limb. *Mech. Dev.*, **77**, 197–200.
16. Swiatek, P.J., Lindsell, C.E., Franco del Amo, F., Weinmaster, G. and Gridley, T. (1994) *Notch1* is essential for postimplantation development in mice. *Genes Dev.*, **8**, 707–719.
17. Conlon, R.A., Reaume, A.G. and Rossant, J. (1995) Notch1 is required for the coordinate segmentation of somites. *Development*, **121**, 1533–1545.
18. Hrabé de Angelis, M., McIntyre, J. and Gossler, A. (1997) Maintenance of somite borders in mice requires the *Delta* homologue *Dll1*. *Nature*, **386**, 717–721.
19. Kusumi, K., Sun, E., Kerrebrock, A.W., Bronson, R.T., Chi, D.-C., Bulotsky, M.S., Spencer, J.B., Birren, B.W., Frankel, W.N. and Lander, E.S. (1998) The mouse pudgy mutation disrupts *Delta* homologue *Dll3* and initiation of early somite boundaries. *Nature Genet.*, **19**, 274–278.
20. Evrard, Y.A., Lun, Y., Aulehla, A., Gan, L. and Johnson, R.L. (1998) *Lunatic fringe* is an essential mediator of somite segmentation and patterning. *Nature*, **394**, 377–381.
21. Zhang, N. and Gridley, T. (1998) Defects in somite formation in *Lunatic fringe* deficient mice. *Nature*, **394**, 374–377.
22. Cohen, B., Bashirullah, A., Dagnino, L., Campbell, C., Fisher, W.W., Leow, C.C., Whiting, E., Ryan, D., Zinyk, D., Boulianne, G., Hui, C.-C., Gallie, B., Phillips, R.A., Lipshitz, H.D. and Egan, S.E. (1997) Fringe boundaries coincide with Notch-dependent patterning centres in mammals and alter Notch-dependent development in *Drosophila*. *Nature Genet.*, **16**, 283–288.
23. Bettenhausen, B., Hrabé de Angelis, M., Simon, D., Guenet, J.-L. and Gossler, A. (1995) Transient and restricted expression during mouse embryogenesis of *Dll1*, a murine gene closely related to *Drosophila Delta*. *Development*, **121**, 2407–2418.
24. Dunwoodie, S.L., Henrique, D., Harrison, S.M. and Beddington, R.S. (1997) Mouse *Dll3*: a novel divergent *Delta* gene which may complement the function of other *Delta* homologues during early pattern formation in the mouse embryo. *Development*, **124**, 3065–3076.
25. Neidhardt, L.M., Kispert, A. and Herrmann, B.G. (1997) A mouse gene of the paired-related homeobox class expressed in the caudal somite compartment and in the developing vertebral column, kidney and nervous system. *Dev. Genes Evol.*, **207**, 330–339.
26. Hess, E.J., Collins, K.A., Copeland, N.G., Jenkins, N.A. and Wilson, M.C. (1994) Deletion map of the coloboma (*Cm*) locus on mouse Chromosome 2. *Genomics*, **21**, 257–261.
27. Hess, E.J., Collins, K.A. and Wilson, M.C. (1996) Mouse model of hyperkinesis implicates SNAP-25 in behavioral regulation. *J. Neurosci.*, **16**, 3104–3111.
28. Theiler, K. and Varnum, D.S. (1981) Development of coloboma (*Cm*/+), a mutation with anterior lens adhesion. *Anat. Embryol.*, **162**, 121–126.
29. Hanahan, D. (1997) Signaling vascular morphogenesis and maintenance. *Science*, **277**, 48–50.
30. Risau, W. (1997) Mechanisms of angiogenesis. *Nature*, **386**, 671–674.
31. Zimrin, A.B., Pepper, M.S., McMahon, G.A., Nguyen, F., Montesano, R. and Maciag, T. (1996) An antisense oligonucleotide to the notch ligand jagged enhances fibroblast growth factor-induced angiogenesis *in vitro*. *J. Biol. Chem.*, **271**, 32499–32502.
32. Johnston, S.H., Rauskolb, C., Wilson, R., Prabhakaran, B., Irvine, K.D. and Vogt, T.F. (1997) A family of mammalian *Fringe* genes implicated in boundary determination and the *Notch* pathway. *Development*, **124**, 2245–2254.
33. Jiang, R., Lan, Y., Chapman, H.D., Shawber, C., Norton, C.R., Serreze, D.V., Weinmaster, G. and Gridley, T. (1998) Defects in limb, craniofacial and thymic development in Jagged2 mutant mice. *Genes Dev.*, **12**, 1046–1057.
34. Muller, H.J. (1932) Further studies on the nature and causes of gene mutations. In *Proceedings of the 6th International Congress on Genetics*. Vol. 1, pp. 213–255.
35. Lindsell, C.E., Boulter, J., diSibio, G., Gossler, A. and Weinmaster, G. (1996) Expression patterns of *Jagged*, *Delta1*, *Notch1*, *Notch2* and *Notch3* genes identify ligand–receptor pairs that may function in neural development. *Mol. Cell. Neurosci.*, **8**, 14–27.
36. Bao, Z.Z. and Cepko, C.L. (1997) The expression and function of Notch pathway genes in the developing rat eye. *J. Neurosci.*, **17**, 1425–1434.
37. Artavanis-Tsakonas, S., Delidakis, C. and Fehon, R.G. (1991) The Notch locus and the cell biology of neuroblast segregation. *Annu. Rev. Cell Biol.*, **7**, 427–452.
38. Spinner, N.B. and Emanuel, B.S. (1996) Deletions and other structural abnormalities of the autosomes. In Rimoin, D.L., Connor, J.M. and Pyeritz, R.E. (eds), *Emery and Rimoin's Principles and Practice of Medical Genetics*, 3rd Edn. Churchill Livingstone, New York, NY, pp. 999–1025.
39. Soriano, P., Montgomery, C., Geske, R. and Bradley, A. (1991) Targeted disruption of the c-src proto-oncogene leads to osteopetrosis in mice. *Cell*, **64**, 693–702.
40. Mansour, S.L., Thomas, K.R. and Capecchi, M.R. (1988) Disruption of the proto-oncogene int-2 in mouse embryo-derived stem cells: a general strategy for targeting mutations to non-selectable genes. *Nature*, **336**, 348–352.
41. Swiatek, P. and Gridley, T. (1993) Perinatal lethality and defects in hindbrain development in mice homozygous for a targeted mutation of the zinc finger gene Krox20. *Genes Dev.*, **7**, 2071–2084.
42. Gao, X., Copeland, N.G., Gilbert, D.J., Jenkins, N.A. and Gridley, T. (1998) Assignment of the murine *Notch2* and *Notch3* genes to chromosomes 3 and 17. *Genomics*, **49**, 160–161.
43. Rowe, L.B., Nadeau, J.H., Turner, R., Frankel, W.N., Letts, V.A., Eppig, J.T., Ko, M.S., Thurston, S.J. and Birkenmeier, E.H. (1994) Maps from two interspecific backcross DNA panels available as a community genetic mapping resource. *Mamm. Genome*, **5**, 253–274.